IEEE Access
Multidisciplinary | Rapid Review | Open Access Journal

IEEE BROADCAST TECHNOLOGY SOCIETY SECTION

Received 6 October 2022, accepted 21 October 2022, date of publication 26 October 2022, date of current version 3 November 2022.

Digital Object Identifier 10.1109/ACCESS.2022.3217496

RESEARCH ARTICLE

Spectrum Sensing for DTMB-A System Using Accumulated Autocorrelation

YUNCHUAN HUANG[1,2], CHAO ZHANG[1,2,3], (Senior Member, IEEE), AND CHANGYONG PAN[1,2,3], (Senior Member, IEEE)

[1]Department of Electronic Engineering, Tsinghua University, Beijing 100084, China
[2]Beijing National Research Center for Information Science and Technology, Beijing 100084, China
[3]Peng Cheng Laboratory, Shenzhen 518055, China

Corresponding author: Chao Zhang (z_c@tsinghua.edu.cn)

This work was supported in part by the China National Science Foundation under Grant 61931015, in part by the Peng Cheng Laboratory under Grant PCL2021A10, and in part by the Guoqiang Institute of Tsinghua University.

ABSTRACT The digital terrestrial television multimedia broadcasting - advanced (DTMB-A) system demands an accurate and reliable spectrum sensing method for its implementation. In this paper, an effective method based on weighted autocorrelation of the frame headers is proposed for single-node spectrum sensing in DTMB-A. The decision threshold, lower bounds and miss detection rate of the proposed method are researched in detail. Simulation results indicate that the proposed method shows better sensing accuracy and robustness compared with the existing methods under various channels, while the cost of its higher complexity is acceptable. Furthermore, by using piecewise-weighted information fusion, the proposed method is extended into cooperative spectrum sensing to overcome the problems of shading and hidden terminals in networking. Our work ensures the efficiency of spectrum sensing and contributes to the better use of DTMB-A system in future applications.

INDEX TERMS Autocorrelation, DTMB-A, frame headers, information fusion, spectrum sensing.

I. INTRODUCTION

Spectrum sensing is a key technology in cognitive radio (CR), which can detect the real-time information of the spectrum holes, and hence ensure the dynamic distribution and utilization of the spectrum resources. As for digital television, higher spectrum utilization efficiency is crucial owing to its broader applications and lower latency demands [1]. In 2019, the digital terrestrial television multimedia broadcasting - advanced (DTMB-A) was adopted as the latest worldwide standard by International Telecommunications Union (ITU) [2], [3]. In order to support flexible broadcasting and hybrid networking services based on DTMB-A, the spectrum resources will not be allocated for users ahead of time. Therefore, for the better use of spectrum, it is essential to detect the DTMB-A signal accurately even in the low signal-to-noise ratio (SNR) cases.

So far, some practical sensing methods have been proposed for different transmitting standards. Energy detector based sensing (EDBS) [4] is a simple way for spectrum sensing, which predicts the existence of the spectrum holes according to the energy of the measured signals without any prior information. However, the detection accuracy of EDBS is fairly terrible than other specialized methods because it neglects the specific features of signals. Besides, it cannot distinguish the primary user and the interferences. Matched filter or cross-correlation is another practical spectrum sensing method which relies on known pilot sequences. This approach has been proved to be optimal under maximum likelihood ratio when the prior information of the detected signal is known to users. But when there are interferences like multipath effects or carrier frequency offset (CFO) [5], [6], its performance will deteriorate seriously. A typical example of cross-correlation methods is the pseudo-noise cross correlation (PNCC) proposed in [7]. The delayed autocorrelation method was introduced in [8] to detect the primary users for DVB-T system, as it's an effective way applicable to the cyclic-prefix orthogonal frequency division multiplexing (CP-OFDM) systems. Moreover, the advantages of autocorrelation based methods are studied in [9] for OFDM-like systems, which

The associate editor coordinating the review of this manuscript and approving it for publication was Wei Li.

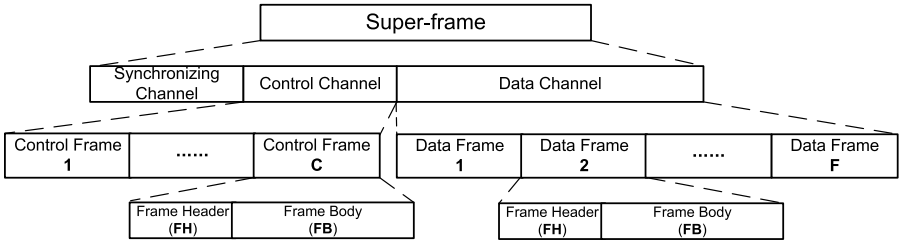

FIGURE 1. The frame structure of DTMB-A.

show better performance than the energy detector, covariance detector [10] and cyclostationary correlation detector [11]. In order to overcome the CFO effects, [12] proposed an improved covariance detector, but it requires rather additional complexity and cannot distinguish the primary user as well. [13] improved the cyclostationary correlation detector to combat the CFO and clock impairments with the extra offline optimization. The method in [14] uses approximated likelihood ratio test (ALRT) and CFO compensation for DVB-T standards. However, considering that DTMB series adopt time domain synchronization - OFDM (TDS-OFDM), the frame structure and guard interval are quite different from other digital terrestrial television broadcasting standards like ATSC [15] and DVB-T. For DTMB systems, some related work focused on pseudo-noise autocorrelation (PNAC) [16], [17]. However, there is still no existing method applied directly to DTMB-A.

Given the above considerations, we proposed an effective new algorithm named different interval pseudo-noise autocorrelation (DIPNAC) for spectrum sensing in DTMB-A system. The new method allows for the frame structure unique to DTMB-A, so that it can make fully use of the sensed signals by accumulating the correlation results within different intervals. Besides, owing to the intrinsic non-coherent property of autocorrelation, the new scheme is bound to be robust against the CFO and the multipath effects in channels. Furthermore, to overcome the problems like shading and hidden terminals in CR systems, this new method is expanded into cooperative spectrum sensing based on piecewise-weighted information fusion, in which different types of piecewise coefficients are designed for varied scenarios. This paper gives detailed description about the new method, including the sensing procedures, the theoretical performance and the computational complexity. According to Neyman-Pearson detection theorem, the simulation results and receiver operator characteristics (ROC) are demonstrated to testify the effectiveness. The previous related work is introduced in [18], nevertheless, more comprehensive analysis and simulation results are demonstrated in this paper.

The following part of this paper contains 5 sections. In Section II, we will introduce the model of spectrum sensing in DTMB-A. Section III presents the detailed description of DIPNAC, including the theoretical inferences and the performance estimation. Section IV expands DIPNAC from the single node detection into cooperative spectrum sensing. Simulation results related will be demonstrated and analysed in Section V. In the end, a comprehensive conclusion of this paper will be given in Section VI.

II. SYSTEM MODEL

A. THE FRAME STRUCTURE OF DTMB-A

The frame structure of the DTMB-A system is shown in Fig. 1. The DTMB-A signal is divided into super-frames in physical layer with a symbol rate of 7.56 MHz for 8MHz bandwidth mode [3]. Each super-frame contains the synchronizing channel, data channel and control channel. The signal frames in data channel and control channel share the same frame structure, which is composed of the frame header (FH) and the frame body (FB).

The FH of each signal frame comprises a multi-carrier pseudo-noise (PN-MC) sequence in $2K$ sample length, where K can be chosen from 256, 512 and 1024. The length of FB is N samples, where N can be 4096, 8192 and 32768 according to different scenarios. It is noteworthy that the PN-MC sequences in FH are generated through replacement and inverse discrete Fourier transform (IDFT) from frequency-domain binary PN sequences, which are used as guard intervals for synchronization and channel estimation at the receiver. FH and FB have the same average energy in all working modes.

B. SPECTRUM SENSING FOR DTMB-A

Here, we use $x[n]$ to denote the DTMB-A signal to be transmitted through the channel. As mentioned above, the length of FH, FB and the signal frame can be denoted as L, N and M, respectively. It is obvious that $M = L+N$ and the average energy of the signal $\sigma_p^2 = E\{x[n]x^*[n]\}$. Considering the transmitting environments, the received signal $r[n]$ is always interfered by the noise and CFO effects. Therefore, we use hypothesis $\mathcal{H}_0$ to indicate there is only noise in $r[n]$ and H_1 for both the useful signal and noise received in $r[n]$:

$$\begin{cases} \mathcal{H}_0 : r[n] = w[n] \\ \mathcal{H}_1 : r[n] = e^{j(2\pi f_\Delta n+\theta_0)}x[n] + w[n] \end{cases} \tag{1}$$

where f_Δ is the normalized CFO factor and θ_0 is the initial phase of the signal. $w[n]$ represents the noise in channel which is a complex Gaussian variable with $w[n] \sim \mathcal{CN}(0, \sigma_w^2)$.

In CR systems, the primary users have the authorization to access the licensed bands without any preprocessing, whereas the secondary users can access only when the spectrum resources are not occupied. For secondary users, the target of spectrum sensing is to decide which hypothesis above to be accepted based on the receiving signal. Since the symbol rate, the bandwidth and three FH modes of the system are known to secondary users beforehand, the correlation-based spectrum sensing methods assume arbitrary starting position of FH within an entire frame length M, and calculate the correlation results under those assumptions to achieve the decision statistic finally.

C. A REVIEW ON PNCC AND PNAC

Since a lot of work has focused on spectrum sensing in DTMB, before the demonstration of our work, it is obliged to introduce the following typical two methods, i.e. PNAC and PNCC.

1) PSEUDO-NOISE AUTOCORRELATION (PNAC)

PNAC makes use of the autocorrelation results between the adjacent FHs. The decision statistic $t_{\mathrm{PNAC}}(m)$ is obtained as:

$$t_{\mathrm{PNAC}}(m) = \frac{1}{S}\sum_{s=0}^{S-1} R(m, s) \tag{2}$$

where, S represents the number of involved correlation results, and $R(m, s)$ is given in the form:

$$R(m, s) = \frac{1}{L}\sum_{n=0}^{L-1} r[m+n+sM]r^*[m+n+(s+1)M] \tag{3}$$

According to the central limit theorem, $t_{\mathrm{PNAC}}(m)$ is a complex Gaussian variable when S is large enough. Under hypothesis $\mathcal{H}_0$, the mean of $t_{\mathrm{PNAC}}(m)$ is zero and the variance $\sigma^2_{\mathrm{PNAC},0} = \sigma_w^4/SL$. Under hypothesis $\mathcal{H}_1$, $t_{\mathrm{PNAC}}(m) \sim \mathcal{CN}(\mu_1, \sigma^2_{\mathrm{PNAC},1})$, where:

$$\begin{cases} \mu_1 = \sigma_p^2 \\ \sigma^2_{\mathrm{PNAC},1} = \dfrac{2\sigma_p^2\sigma_w^2 + \sigma_w^4}{SL} \end{cases} \tag{4}$$

The decision statistic T_{PNAC} and the threshold under the false alarm rate P_{FA} are given by:

$$\begin{cases} T_{\mathrm{PNAC}} = \max\limits_{0\le m<M} |t_{\mathrm{PNAC}}(m)| \\ \gamma_{T,\mathrm{PNAC}} = \left(-\sigma^2_{\mathrm{PNAC},0}\ln\left(1-(1-P_{\mathrm{FA}})^{\frac{1}{M}}\right)\right)^{\frac{1}{2}} \end{cases} \tag{5}$$

PNAC is robust against the CFO and the multipath effects because of the non-coherent property of autocorrelation. However, the sensing performance is undesirable under low SNR region.

2) PSEUDO-NOISE CROSS CORRELATION (PNCC)

In PNCC, the cross correlations between the FH and the local PN-MC sequences are calculated and averaged to obtain $t_{\mathrm{PNCC}}(m)$:

$$R_{\mathrm{PNCC}}(m) = \frac{1}{L}\sum_{n=0}^{L-1} r[m+n]c^*[n] \tag{6}$$

$$t_{\mathrm{PNCC}}(m) = \frac{1}{S}\sum_{s=0}^{S-1} |R_{\mathrm{PNCC}}(m+sM)|^2 \tag{7}$$

where $c[n]$ is the normalized local PN-MC sequence. When L is large enough, $t_{\mathrm{PNCC}}(m)$ follows the central and non-central Chi-squared distributions with the degree of freedom of $2S$ under $\mathcal{H}_0$ and $\mathcal{H}_1$, respectively. The decision statistic and the threshold are given by:

$$\begin{cases} T_{\mathrm{PNCC}} = \max\limits_{0\le m<M} |t_{\mathrm{PNCC}}(m)| \\ \gamma_{T,\mathrm{PNCC}} = \dfrac{\sigma_w^2}{2S} Q^{-1}_{2S}\left(1-(1-P_{\mathrm{FA}})^{\frac{1}{M}}\right) \end{cases} \tag{8}$$

where $Q^{-1}_{2S}(\cdot)$ is the inverse function of the right-tail probability of non-central Chi-square distribution with degrees of freedom equal to $2S$.

PNCC has the better sensing performance than PNAC, especially over AWGN channel. But it is sensitive to multipath and CFO effects. Besides, the cross-correlation operation requires additional complexity in practice than autocorrelation, so PNCC cannot meet the demands in complex transmitting environments.

III. THE PROPOSED DIPNAC METHOD

In this section, we will discuss the improved method of spectrum sensing in DTMB-A. On one hand, we want to retain the property of robustness in PNAC. On the other hand, considering that PNAC only makes use of the adjacent FHs to obtain the decision statistic, the performance is bound to be improved if the correlation results of FH with different intervals are counted in. Therefore, we'd like to investigate the distribution of the accumulated autocorrelation results of the FHs firstly. Afterwards, the coefficients of the results are optimized in order to maximize the difference of the decision statistic between $\mathcal{H}_0$ and $\mathcal{H}_1$. Based on Neyman-Pearson theorem, the threshold will be designed under a given false alarm rate. Next, the theoretical performance of DIPNAC detector will be analysed, including the lower bounds of miss detection rate and the ROCs. Finally, we will compare the complexity of DIPNAC with the existing methods.

A. THE DISTRIBUTION OF ACCUMULATED AUTOCORRELATION

Note that in the Eq. (3), the result is obtained by averaging the correlation of adjacent FHs with frame index s and $s+1$. Actually, the correlation results of FHs with different

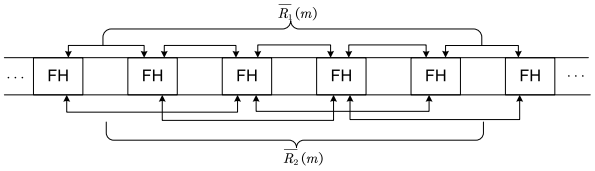

FIGURE 2. The accumulated autocorrelation $\overline{R_d}(m)$ within gap d.

intervals can be expressed as:

$$R_d(m;k)=\frac{1}{L}\sum_{n=0}^{L-1} r[m+n+kM]r^*[m+n+(k+d)M] \tag{9}$$

where $R_d(m;k)$ is used to denote the autocorrelation between the received signal with frame index offset k and its delayed version with the interval equal to d. The correlation length is L corresponding to FH. Substitute the $r[n]$ under $\mathcal{H}_1$ to (9), then average all the $R_d(m;k)$ with the same d during the sensing time:

$$\overline{R_d}(m)=\frac{1}{S_d}\sum_{k=0}^{S_d-1} R_d(m;k)=e_d X_d(m)+W_d(m) \tag{10}$$

Figure 2 illustrates the procedure of computing the $\overline{R_d}(m)$ within different values of d. In Eq. (10), $S_d = F - d$ is the number of $R_d(m)$ involved, and F is the total number of the sensed frames. $e_d = e^{-2\pi f_\Delta Md}$ is the phase rotation factor and depends merely on d. $X_d(m)$ is the autocorrelation function of $x[\cdot]$:

$$X_d(m)=\frac{1}{S_d L}\sum_{s=0}^{S_d-1}\sum_{n=0}^{L-1} x[n+m+sM]x^*[n+m+(s+d)M] \tag{11}$$

and $W_d(m)$ is the autocorrelation function of the noise $w[\cdot]$:

$$W_d(m)=\frac{1}{S_d L}\sum_{s=0}^{S_d-1}\sum_{n=0}^{L-1} w[n+m+sM]w^*[n+m+(s+d)M] \tag{12}$$

The cross-terms between $x[\cdot]$ and $w[\cdot]$ are omitted in equation (10) in view that the signal and the noise are statistically independent.

According to the central limit theorem, $W_d(m)$ is a complex Gaussian variable when the value of S_d is large enough, denoted as:

$$W_d(m)\sim\mathcal{CN}(0,\frac{1}{S_d L}\sigma_w^4) \tag{13}$$

In PNAC, only $\overline{R_1}(m)$ contributes to the final decision statistic, which neglects other available information of signal during the sensing time, so the sensing performance of PNAC is limited. However, by averaging the correlation results $\overline{R_d}(m)$ within different d properly, the new method makes better use of the information during the sensing time in order to achieve greater detection statistic than PNAC, which gives rise to remarkable advances in sensing performance.

So far, we can obtain the accumulated correlation results by combining $\overline{R_d}(m)$ with different d appropriately. Actually, $\overline{R_d}(m)$ cannot be directly summed up as the decision statistic because it contains a phase rotation factor e_d. In order to avoid the potential loss, a new variable is introduced as $U_d(m) = \overline{R_d}(m)\,\overline{R_{d+1}}^*(m)$:

$$\begin{aligned} U_d(m) &= \overline{R_d}(m)\,\overline{R_{d+1}}^*(m) \\ &= X_d X_{d+1}^* + e_d X_d W_{d+1}^* + e_{d+1} X_{d+1}^* W_d + W_d W_{d+1}^* \end{aligned} \tag{14}$$

The mean and variance of $U_d(m)$ can be calculated as:

$$\begin{cases} E[U_d(m)] &= \sigma_p^4 \\ var[U_d(m)] &= \dfrac{\sigma_w^8}{S_d S_{d+1} L^2}+\dfrac{\sigma_p^4\sigma_w^4}{S_d L}+\dfrac{\sigma_p^4\sigma_w^4}{S_{d+1}L} \end{cases} \tag{15}$$

By combining the $U_d(m)$s with different d linearly, we have:

$$t_{\mathrm{DIPNAC}}(m)=\sum_{d=1}^{D}\lambda_d U_d(m) \tag{16}$$

where, D is the number of involved U_d, and λ_d is the coefficient, which will be optimized afterwards. Here we assume that $\sum_{d=1}^{D}\lambda_d = 1$ for normalization requirements. According to the central limit theorem, t_{DIPNAC} is a complex Gaussian variable under the hypothesis $\mathcal{H}_1$ when the involved correlation results are large enough:

$$t_{\mathrm{DIPNAC}}(m)|\mathcal{H}_1\sim\mathcal{CN}(\mu_1,\sigma_1^2) \tag{17}$$

and

$$\begin{cases} \mu_1=\sigma_p^4\sum\limits_{d=1}^{D}\lambda_d \\ \sigma_1^2=\sum\limits_{d=1}^{D}\lambda_d^2\left(\dfrac{\sigma_w^8}{S_d S_{d+1}L^2}+\dfrac{\sigma_p^4\sigma_w^4}{S_d L}+\dfrac{\sigma_p^4\sigma_w^4}{S_{d+1}L}\right) \end{cases} \tag{18}$$

In fact, $t_{\mathrm{DIPNAC}}(m)$ is also a complex Gaussian variable under $\mathcal{H}_0$, while the mean will be zero, and the variance σ_0^2 will be simplified as:

$$\sigma_0^2=\sum_{d=1}^{D}\lambda_d^2\frac{\sigma_w^8}{S_d S_{d+1}L^2} \tag{19}$$

B. THE OPTIMIZATION OF DECISION STATISTIC

As mentioned above, $t_{\mathrm{DIPNAC}}(m)$ is a complex Gaussian variable under both $\mathcal{H}_0$ and $\mathcal{H}_1$. However, in order to attain the decision statistic, the coefficients λ_d should be optimized. The target is to maximize the difference between $t_{\mathrm{DIPNAC}}(m)|\mathcal{H}_1$ and $t_{\mathrm{DIPNAC}}(m)|\mathcal{H}_0$, so that they can be easily distinguished.

In information theory, the Kullback-Leibler (KL) divergence, also known as the relative entropy, can be used to measure the degree of dissimilarity between two random

variables with continuous probability distributions $p_1(x)$ and $p_0(x)$ respectively:

$$KL(p_1||p_0) = \int p_1(x) \ln \frac{p_1(x)}{p_0(x)} dx \tag{20}$$

With regard to our situations, we will introduce the KL divergence between $t_{\mathrm{DIPNAC}}(m)|\mathcal{H}_1$ and $t_{\mathrm{DIPNAC}}(m)|\mathcal{H}_0$ as the optimizing criterion, which is computed by:

$$KL(\mathcal{H}_1||\mathcal{H}_0) = \ln \frac{\sigma_0^2}{\sigma_1^2} + \frac{|\mu_1^2|}{\sigma_0^2} + \frac{\sigma_1^2}{\sigma_0^2} - 1 \tag{21}$$

Consider that when SNR is very low in most scenarios, i.e. $\sigma_p^2 \ll \sigma_w^2$, the approximation holds that $\sigma_0^2 \approx \sigma_1^2$. Equation (21) can be rewritten as:

$$\begin{aligned} KL(\mathcal{H}_1||\mathcal{H}_0) &= \ln \frac{\sigma_0^2}{\sigma_1^2} + \frac{|\mu_1^2|}{\sigma_0^2} + \frac{\sigma_1^2}{\sigma_0^2} - 1 \overset{\sigma_0^2 \approx \sigma_1^2}{\approx} \frac{|\mu_1^2|}{\sigma_0^2} \\ &= \frac{\left|\sigma_p^4 \sum_{d=1}^{D} \lambda_d\right|^2}{\sum_{d=1}^{D} \lambda_d^2 \frac{\sigma_w^8}{S_d S_{d+1} L^2}} \\ &= \frac{L^2}{\sigma_w^8} \cdot \frac{\left|\sigma_p^4 \sum_{d=1}^{D} \lambda_d\right|^2}{\sum_{d=1}^{D} \frac{\lambda_d^2}{S_d S_{d+1}}} \end{aligned} \tag{22}$$

Assume that $\sum_{d=1}^{D} \lambda_d = 1$, the numerator of the last fraction in Eq. (22) is a constant. Now, in order to maximize the value of $KL(\mathcal{H}_1||\mathcal{H}_0)$, the problem could be simplified to only minimize the value of

$$G(\lambda_d) = \sum_{d=1}^{D} \lambda_d^2 / S_d S_{d+1} \tag{23}$$

under the constraint $\sum_{d=1}^{D} \lambda_d = 1$. Obviously $G(\cdot)$ is a convex function of λ_d, $d = 1, 2, \ldots, D$ and the global minimum is unique. Construct the Lagrangian function $\varphi(\lambda_d)$:

$$\varphi(\lambda_d) = G(\lambda_d) - C \cdot \left(\sum_{d=1}^{D} \lambda_d - 1\right) \tag{24}$$

Let the derivative of $\varphi(\cdot)$ be zero, we have:

$$\begin{aligned} \frac{\partial \varphi(\lambda_d)}{\partial \lambda_d} &= 2\lambda_d / S_d S_{d+1} - C = 0 \\ &\Rightarrow \begin{cases} \lambda_d = \dfrac{C}{2} S_d S_{d+1} \\ C = \dfrac{2}{\sum_{d=1}^{D} S_d S_{d+1}} \end{cases} \end{aligned} \tag{25}$$

Consequently, we have found the optimum decision statistic of DIPNAC, rewritten as:

$$\begin{aligned} T_{\mathrm{DIPNAC}} &= \max_{0 \leqslant m < M} |t_{\mathrm{DIPNAC}}(m)| \\ &= \max_{0 \leqslant m < M} \left| \sum_{d=1}^{D} \frac{C}{2} S_d S_{d+1} U_d(m) \right| \end{aligned} \tag{26}$$

where $C = \dfrac{2}{\sum_{d=1}^{D} S_d S_{d+1}}$ in Eq. (26).

It can be witnessed that DIPNAC algorithm inherits the non-coherent property of PNAC, as they both rely on the autocorrelation results to obtain the final decision statistic. Therefore, they are bound to be robust against the CFO and multipath effects, compared with the PNCC method. When $D = 1$, DIPNAC will degenerate into PNAC for only the adjacent FH autocorrelation results count in. In general conditions for $D > 1$, more accumulated FH autocorrelation results are used in DIPNAC to obtain the greater decision statistic for detection and enhance the sensing performance.

C. THE DECISION THRESHOLD AND THEORETICAL PERFORMANCE

According to Neyman-Pearson theorem, the threshold γ_T should be set to ensure that the miss detection rate to be minimized, while the false alarm rate P_{FA} remains unchanged:

$$\int_{\gamma_T}^{\infty} f_{T_{\mathrm{DIPNAC}}}(x|\mathcal{H}_0)\, dx = P_{\mathrm{FA}} \tag{27}$$

where $f_{T_{\mathrm{DIPNAC}}}(x|\mathcal{H}_0)$ is the probability density function (pdf) of the decision statistic T_{DIPNAC} under $\mathcal{H}_0$.

Under hypothesis $\mathcal{H}_0$, $t_{\mathrm{DIPNAC}}(m)$ is a zero-mean complex Gaussian variable, and $|t_{\mathrm{DIPNAC}}(m)|$ follows the Rayleigh distribution. Thus, T_{DIPNAC} follows a joint Rayleigh distribution, which is difficult to figure out the exact pdf expressions. Assume that $|t_{\mathrm{DIPNAC}}(m)|$ in different m is independent and identically distributed (i.i.d), hence:

$$\begin{aligned} P\{T_{\mathrm{DIPNAC}}(m) < t_0|\mathcal{H}_0\} &\approx \prod_{m=0}^{M-1} P\{|t_{\mathrm{DIPNAC}}(m)|\mathcal{H}_0| < t_0\} \\ &= \left(1 - e^{-\frac{t_0^2}{\sigma_0^2}}\right)^M \end{aligned} \tag{28}$$

Therefore, we can obtain the decision threshold γ_T of DIPNAC under a given false alarm rate P_{FA}:

$$\gamma_T = \left(-\sigma_0^2 \ln\left(1 - (1 - P_{\mathrm{FA}})^{\frac{1}{M}}\right)\right)^{\frac{1}{2}} \tag{29}$$

Under hypothesis $\mathcal{H}_1$, $t_{\mathrm{DIPNAC}}(m)$ is still a complex Gaussian variable, but the magnitude $|t_{\mathrm{DIPNAC}}(m)|$ follows the Ricean distribution. Given a decision threshold γ_T, we can obtain a lower bound of miss detection rate P_{MD} by calculating the value of the cumulative distribution function:

$$P_{\mathrm{MD}} \approx 1 - Q_1\left(\frac{\mu_1}{\sigma_1}, \frac{\gamma_T}{\sigma_1}\right) \tag{30}$$

where $Q_1(\alpha, \beta)$ is the Marcum Q function in the form:

$$Q_1(\alpha, \beta) = \int_{\beta}^{\infty} x \exp\left(-\frac{x^2 + \alpha^2}{2}\right) I_0(\alpha x) dx \tag{31}$$

and $I_0(x)$ is the modified zero-order Bessel function of the first kind.

TABLE 1. Complexity comparison (F is the number of sensed frames).

Algorithm	Complexity
EDBS	FM
PNAC	$(F-1)L+(F-1)(M-1)$
PNCC	FLM
DIPNAC	$D(F-1)L+D(F-1)(M-1)$

Additionally, the ROC of DIPNAC detector can be estimated according to:

$$P_{\mathrm{D}} \approx Q_1\left(\frac{\mu_1}{\sigma_1}, \frac{\left(-\sigma_0^2 \ln\left(1-(1-P_{\mathrm{FA}})^{\frac{1}{M}}\right)\right)^{\frac{1}{2}}}{\sigma_1}\right) \tag{32}$$

where, P_{D} is the detection rate and P_{FA} is the pre-defined false alarm rate.

D. COMPLEXITY ANALYSIS

The complexity comparison is evaluated by the times of the complex multiplications of each method, which is given in Table 1. It is dear that EDBS has the lowest complexity among the sensing methods. However, the terrible performance of EDBS renders it incompetent for higher sensing requirements.

Autocorrelation can make use of the result produced in last iteration in hardware implementation, while the cross-correlation must process the complex multiplications independently at each step. Therefore, the complexity of PNCC is remarkably higher than that of PNAC. Besides, DIPNAC has the medium complexity among all of the sensing methods. In fact, DIPNAC makes a trade-off between the sensing performance and the complexity by using a parameter D. With an acceptable cost additionally in complexity, it contributes to better use of the spectrum resources.

IV. DIPNAC BASED COOPERATIVE SENSING

A. COOPERATIVE SENSING AND INFORMATION FUSION

In CR systems, there are some limitations for single node spectrum sensing due to the shading, multipath effect and hidden terminal problems. Therefore, cooperative sensing using the information from different nodes is proposed to obtain reliable sensing results [19], [20], [21], [22]. Assume that each node in cooperative sensing uses the DIPNAC detector to complete the sensing procedures independently. The information from each node should be gathered and combined according to some specific rules, so that the final decision statistics are loyal to the facts. Hence, the single node DIPNAC detector is expanded into cooperative sensing, and the effective rule of information fusion will be studied.

The easiest way of combination is the equal gain combining (EGC), which assumes that all the nodes involved have the same reliability [19]. To overcome the problem of hidden terminals, the more effective way is to modify the weight of each node according to their statuses, while it requires more prior information of the node, such as the SNR and the distance. However, it is difficult to make a precise estimation about the SNR or distance under complicated sensing environments. In view that the approximate distribution of the decision statistic T_{DIPNAC} has been obtained, a piecewise-weighted information fusion strategy is proposed here, where the weights depend merely on the distribution and the decision statistic sensed by each node.

B. THE PIECEWISE-WEIGHTED COOPERATIVE SENSING

Assume that the number of the nodes involved in the sensing network is N_{css}, and the DIPNAC decision statistic of each node is T_i, $i = 0, 1, \ldots, N_{\mathrm{css}}-1$. The final decision statistic after combination could be denoted as:

$$T_{\mathrm{coop}} = \frac{1}{\sum_{i=0}^{N_{\mathrm{css}}-1} w_i} \sum_{i=0}^{N_{\mathrm{css}}-1} w_i T_i \tag{33}$$

where w_i is the weighting coefficient. Intuitively, the reliable nodes should be allocated with larger weights, while unreliable nodes should have lower weights in order to alleviate their effects.

Consider the probability distribution of the decision statistic T_i, as mentioned in Eq. (28):

$$\begin{aligned} P\{T_i < t_0|\mathcal{H}_0\} &\approx \prod_{m=0}^{M} P\left(|t_{\mathrm{DIPNAC}}| < t_0\right) \\ &= \left(1-\exp\left(-\frac{t_0^2}{\sigma_0^2}\right)\right)^M \end{aligned} \tag{34}$$

Hence the pdf of T_i under $\mathcal{H}_0$ could be obtained by calculating the derivative:

$$f_{T_i}(t_0|\mathcal{H}_0) = \frac{2Mt_0}{\sigma_0^2}\left(1-\exp\left(-\frac{t_0^2}{\sigma_0^2}\right)\right)^{M-1}\exp\left(-\frac{t_0^2}{\sigma_0^2}\right) \tag{35}$$

Under $\mathcal{H}_1$, T_i follows the Ricean distribution, and the pdf could be given as:

$$f_{T_i}(t_0|\mathcal{H}_1) = \frac{t_0}{\sigma_1^2}\exp\left(-\frac{\left(t_0^2+\mu_1^2\right)}{2\sigma_1^2}\right) I_0\left(\frac{t_0\mu_1}{\sigma_1^2}\right) \tag{36}$$

In the applications of spectrum sensing, because of the low SNR in specific receiving environments, it is difficult to obtain the precise value for Eq. (36) because the estimation of the signal power σ_p^2 might be inaccurate. However, the noise power σ_w^2 can be estimated from the environment. Considering that σ_0^2 depends only on σ_w^2, the coefficient w_i could be modified according to the distribution under $\mathcal{H}_0$ preferably. The task of cooperative sensing is to lower the miss detection rate while maintaining the level of the false alarm rate. It is worthwhile to look into the effects of w_i on the decision statistics under both $\mathcal{H}_0$ and $\mathcal{H}_1$.

Under $\mathcal{H}_0$, the power of signal is zero in light that no signals are transmitted, and there is no difference between the nodes' reliability. Hence, the weighting coefficients should be the same accordingly. Under $\mathcal{H}_1$, it is obvious that the

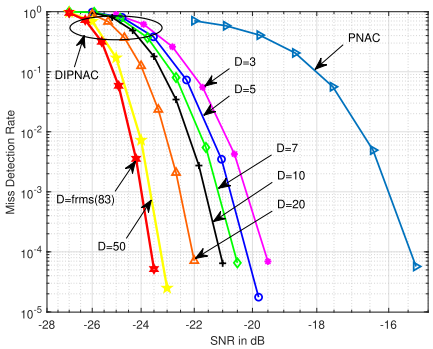

FIGURE 3. The ideal performance of DIPNAC (number of frames = 83).

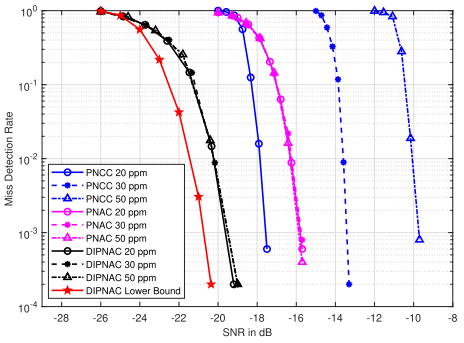

FIGURE 4. The performance comparison over AWGN channel.

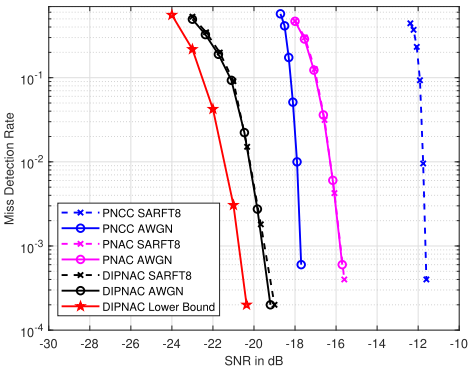

FIGURE 5. The performance comparison over SARFT 8 channel.

TABLE 2. The numerical comparison of decision threshold.

D	3	5	7	10	20
γ_T	1.27	1.48	1.66	1.88	2.39
γ_T^*	1.34	1.61	1.70	1.89	2.36

nodes in high SNR environments should be allocated with larger weights. However, the precise estimation of SNR is hard to obtain as mentioned above. Considering that higher SNR contributes to larger decision statistic T_i, which is less likely to happen under $\mathcal{H}_0$, so the metrics of reliability could be designed according to the value of T_i or its distribution in Eq. (35).

Based on the considerations above, two kinds of weighting coefficients strategy are proposed here:

- Strategy A: piecewise weighting coefficients based on the decision statistics

$$w_{A,i} = \begin{cases} T_i, & T_i > \gamma_0 \\ \gamma_0, & T_i \le \gamma_0 \end{cases} \tag{37}$$

- Strategy B: piecewise weighting coefficients based on the probability distribution

$$w_{B,i} = \begin{cases} \dfrac{1}{f_{T_i}(T_i|\mathcal{H}_0)}, & T_i > \gamma_0 \\ \dfrac{1}{f_{T_i}(\gamma_0|\mathcal{H}_0)}, & T_i \le \gamma_0 \end{cases} \tag{38}$$

where γ_0 is the decision threshold in single node sensing, as given in Eq. (29).

V. SIMULATION RESULTS

A. THE PERFORMANCE OF DIPNAC IN SINGLE NODE SENSING

The parameters for the simulation are set according to [17]. The sensing time is 50 ms, which contains 83 frames of DTMB-A signals. The CFO normalization factor is 800MHz, and the false alarm rate is set to be fixed on 0.01. All simulations were performed in Matlab R2019b for 5000 times as to FH 512 mode in DTMB-A ($K = 256$).

First, the setting of decision threshold over AWGN channel is validated for DIPNAC. On the one hand, the theoretical threshold γ_T obtained by Eq. (29) is computed for different D with target false alarm probability $P_{\text{FA}} = 0.01$. On the other hand, by computing the empirical distribution of T_{DIPNAC} under hypothesis $\mathcal{H}_0$ in simulation, the accurate decision threshold γ_T^* with the same false alarm probability could be obtained as a reference. The results are shown in Table 2.

The ideal performance of DIPNAC detectors under the AWGN channel with different parameter D is shown in Fig. 3. All the detectors use 83 signal frames during the sensing time to make the decision. The horizontal axis represents the SNR in dB, and the vertical axis reflects the miss detection rate. The lower curve indicates the better sensing performance in the same environment. It is obvious that DIPNAC outperforms the original PNAC method. Furthermore, the larger value of D contributes to the better sensing performance, but this improvement is not linearly increasing with D. When D approaches the number of sensed frames F, the gain in performance will be almost distinguishable. Considering that the larger D may cause an extra cost in complexity, users should select the optimum value of D to meet their requirements in practice.

The performance comparison between DIPNAC and the exiting methods of PNAC and PNCC over AWGN channel is illustrated in Fig. 4, in which $D = 5$ is adopted for DIPNAC. The CFO is set to be 20 parts per million (ppm),30 and 50 ppm respectively in simulation. It is obvious from Fig. 4 the practical DIPNAC detector has the best sensing performance than the other two detectors. When the miss detection rate achieves

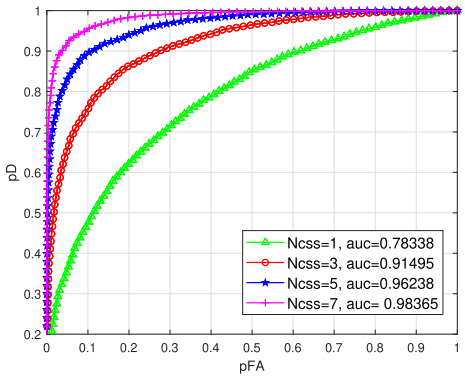

FIGURE 6. The ROCs of DIPNAC cooperative sensing (EGC).

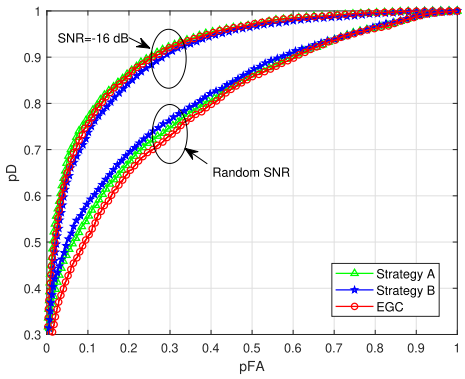

FIGURE 7. The ROC comparison of strategies with constant and random SNR.

10^{-3} level, DIPNAC leads about 2.05 dB than PNCC with 20 ppm CFO, about 3.81 dB than PNAC, and about 6.20 dB than PNCC with 30 ppm CFO. It can be found that PNCC will suffer from an obvious deterioration in performance when the CFO increase to 50 ppm, while the curves of DIPNAC and PNAC remain nearly unchanged, which shows the robustness of DIPNAC detector against the CFO.

The sensing performance over SARFT (State Administration of Radio Film and Television of China) 8 channel [23] is given in Fig. 5. SARFT 8 is a typical multipath channel widely used in single frequency networks, which contains a long-delay echo with power 0 dB. All detectors are set with 20 ppm CFO, and the results over AWGN channel are given in parallel for comparison. Note that DIPNAC still outperforms other detectors under the SARFT channel, which leads about 3.78 dB than PNAC, about 7.94 dB than PNCC when the miss detection rate is at 10^{-3} level. Besides, DIPNAC is still robust against the multipath effects because the changes of the curves are very slight. In contrast, PNCC suffers from a severe deterioration when it works under the multipath channel.

To sum up, the proposed DIPNAC method works efficiently under both the AWGN and the multipath channels. It shows better sensing performance as well as the robustness against the CFO and the multipath effects. Accordingly, we can learn that it uses acceptable extra complexity to obtain an apparent improvement to the sensing performance.

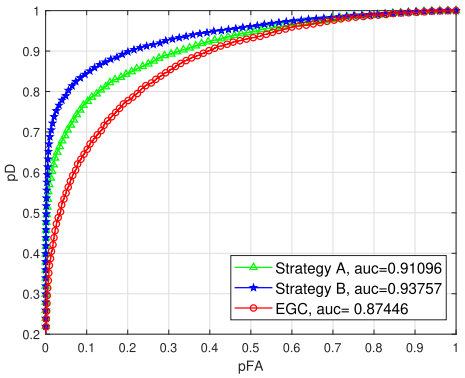

FIGURE 8. The ROC comparison of strategies with the hidden terminal.

B. THE PERFORMANCE OF DIPNAC IN COOPERATIVE SENSING

In this subsection, the simulation results related are given to illustrate the effects of our proposed combining strategies for cooperative sensing, especially for the comparison with EGC. The sensing time is set to be 5 ms and the CFO is 20 ppm for all simulations below. Every node performs the DIPNAC detector independently under the i.i.d AWGN channels [24], [25] in simulation.

Figure 6 shows the ROCs of DIPNAC in cooperative sensing with different number of sensing nodes. Here, the horizontal axis represents for the false alarm rate, and the vertical axis is the detection rate. The strategy is EGC, and the SNR is -16 dB, with other parameters identical to the simulation in single node sensing. The performance indicator of different curves can be reflected by the value of area under curve (AUC), which is also listed for reference in the figure. Obviously, More nodes involved lead to better sensing performance. The AUC of 7 users is about 0.98, while for 5 and 3 users it is 0.96 and 0.91, respectively. Nevertheless, they remarkably exceeds the single-user strategy (only 0.78), for more users could provide more information reflecting the truth in cooperative sensing.

Figure 7 gives the comparison of different strategies in the form ROC. Here, $N_{\text{css}} = 5$ for all the examples. Figure 7 illustrates that when all nodes are with the same SNR, i.e. -16 dB, all the strategies have similar performances. This is because the reliability of each node in this case is almost equal to others, where EGC is bound to work properly. However, strategy A still outperforms the others by a subtle advantage. Besides, when the SNR of each node is uniformly distributed between -23 and -14 dB, the performance of EGC is already exceeded by our proposed strategy A and B.

In Fig. 8, the hidden terminal problem is considered in spectrum sensing, where there is only one user in -13 dB and others in -22 dB. In this case, strategy B has the best sensing performance, for its AUC value reaches 0.93, followed by strategy A with AUC equal to 0.91. However, the AUC of EGC is only 0.87, which is evidently overshadowed by the proposed strategies.

From the simulations above, it can be concluded that the proposed strategies can effectively enhance the performance of DIPNAC based cooperative sensing than EGC strategy, especially when it comes to the hidden terminal problem, which is of great significance for broadcasting networks.

VI. CONCLUSION

In this paper, the DIPNAC detector for spectrum sensing in DTMB-A systems is proposed, which utilizes the accumulation of autocorrelation results within different intervals to obtain reliable decision statistics. Based on Neyman-Pearson theorem, the detailed procedures of DIPNAC are discussed as well as the decision threshold, the miss detection rate and the complexity. Moreover, we expand the DIPNAC into cooperative sensing by using the piecewise-weighted sensing method, and give two strategies to overcome the hidden terminal problems. The proposed methods above show favorable performances in simulation results, which evidently enhance the spectrum efficiency for DTMB-A system.

REFERENCES

[1] M. El-Hajjar and L. Hanzo, "A survey of digital television broadcast transmission techniques," *IEEE Commun. Surveys Tuts.*, vol. 15, no. 4, pp. 1924–1949, 4th Quart., 2013.
[2] International Telecommunication Union, "Digital terrestrial broadcasting systems," Radiocommun. Sector ITU, Geneva, Switzerland, Tech. Rep. BT.2295-3, 2020.
[3] J. Song, C. Zhang, K. Peng, J. Wang, C. Pan, F. Yang, J. Wang, H. Yang, Y. Xue, Y. Zhang, and Z. Yang, "Key technologies and measurements for DTMB-A system," *IEEE Trans. Broadcast.*, vol. 65, no. 1, pp. 53–64, Mar. 2019.
[4] F. F. Digham, M. S. Alouini, and M. K. Simon, "On the energy detection of unknown signals over fading channels," in *Proc. IEEE Int. Conf. Commun. (ICC)*, vol. 5. May 2003, pp. 3575–3579.
[5] J.-J. Van De Beek, M. Sandell, and P. O. Borjesson, "ML estimation of time and frequency offset in OFDM systems," *IEEE Trans. Signal Process.*, vol. 45, no. 7, pp. 1800–1805, Jul. 1997.
[6] S.-S. Li and S.-M. Phoong, "Blind estimation of multiple carrier frequency offsets in OFDMA uplink systems employing virtual carriers," *IEEE Access*, vol. 8, pp. 2915–2923, 2020.
[7] A. Xu, Q. Shi, Z. Yang, K. Peng, and J. Song, "Spectrum sensing for DTMB system based on PN cross-correlation," in *Proc. IEEE Int. Conf. Commun.*, May 2010, pp. 1–5.
[8] H.-S. Chen, W. Gao, and D. G. Daut, "Spectrum sensing for OFDM systems employing pilot tones and application to DVB-T OFDM," in *Proc. IEEE Int. Conf. Commun.*, May 2008, pp. 3421–3426.
[9] M. Naraghi-Pour and T. Ikuma, "Autocorrelation-based spectrum sensing for cognitive radios," *IEEE Trans. Veh. Technol.*, vol. 59, no. 2, pp. 718–733, Feb. 2010.
[10] Y. Zeng and Y.-C. Liang, "Covariance based signal detections for cognitive radio," in *Proc. 2nd IEEE Int. Symp. New Frontiers Dyn. Spectr. Access Netw.*, Apr. 2007, pp. 202–207.
[11] A. V. Dandawate and G. B. Giannakis, "Statistical tests for presence of cyclostationarity," *IEEE Trans. Signal Process.*, vol. 42, no. 9, pp. 2355–2369, Sep. 1994.
[12] W. Xu, W. Xiang, M. Elkashlan, and H. Mehrpouyan, "Spectrum sensing of OFDM signals in the presence of carrier frequency offset," *IEEE Trans. Veh. Technol.*, vol. 65, no. 8, pp. 6798–6803, Aug. 2016.
[13] E. Rebeiz, P. Urriza, and D. Cabric, "Optimizing wideband cyclostationary spectrum sensing under receiver impairments," *IEEE Trans. Signal Process.*, vol. 61, no. 15, pp. 3931–3943, Aug. 2013.
[14] Y. Zeng, Y.-C. Liang, and T.-H. Pham, "Spectrum sensing for OFDM signals using pilot induced auto-correlations," *IEEE J. Sel. Areas Commun.*, vol. 31, no. 3, pp. 353–363, Mar. 2013.
[15] H.-S. Chen, W. Gao, and D. G. Daut, "Signature based spectrum sensing algorithms for IEEE 802.22 WRAN," in *Proc. IEEE Int. Conf. Commun.*, Jun. 2007, pp. 6487–6492.
[16] H.-S. Chen, W. Gao, and D. G. Daut, "Spectrum sensing for DMB-T systems using PN frame headers," in *Proc. IEEE Int. Conf. Commun.*, May 2008, pp. 4889–4893.
[17] L. Liang, J. Wang, and J. Song, "An improved spectrum sensing method for DTMB system based on PN autocorrelation," *IEICE Trans. Commun.*, vol. 96, no. 6, pp. 1559–1565, 2013.
[18] Y. Huang, C. Zhang, and C. Pan, "A spectrum sensing algorithm for DTMB-A based on accumulated autocorrelation of multiple frames," in *Proc. IEEE Int. Symp. Broadband Multimedia Syst. Broadcast. (BMSB)*, Aug. 2021, pp. 1–5.
[19] H. Guo, W. Jiang, and W. Luo, "Linear soft combination for cooperative spectrum sensing in cognitive radio networks," *IEEE Commun. Lett.*, vol. 21, no. 7, pp. 1573–1576, Jul. 2017.
[20] A. Tohamy, U. S. Mohamed, M. M. Abdellatif, T. A. Khalaf, and M. Abdelraheem, "Cooperative spectrum sensing using maximum a posteriori as a detection technique for dynamic spectrum access networks," *IEEE Access*, vol. 8, pp. 156408–156421, 2020.
[21] X. Liu, M. Guan, X. Zhang, and H. Ding, "Spectrum sensing optimization in an UAV-based cognitive radio," *IEEE Access*, vol. 6, pp. 44002–44009, 2018.
[22] S. Zhang, Y. Wang, P. Wan, J. Zhuang, Y. Zhang, and Y. Li, "Clustering algorithm-based data fusion scheme for robust cooperative spectrum sensing," *IEEE Access*, vol. 8, pp. 5777–5786, 2020.
[23] F. Yang, J. Wang, J. Wang, J. Song, and Z. Yang, "Novel channel estimation method based on PN sequence reconstruction for Chinese DTTB system," *IEEE Trans. Consum. Electron.*, vol. 54, no. 4, pp. 1583–1589, Nov. 2008.
[24] J. Ma, G. Zhao, and Y. Li, "Soft combination and detection for cooperative spectrum sensing in cognitive radio networks," *IEEE Trans. Wireless Commun.*, vol. 7, no. 11, pp. 4502–4507, Nov. 2008.
[25] W. Zhang, Y. Guo, H. Liu, Y. Chen, Z. Wang, and J. Mitola, "Distributed consensus-based weight design for cooperative spectrum sensing," *IEEE Trans. Parallel Distrib. Syst.*, vol. 26, no. 1, pp. 54–64, Jan. 2015.

YUNCHUAN HUANG received the B.S. degree from Southeast University, in 2020. He is currently pursuing the master's degree with the Department of Electronic Engineering, Tsinghua University. His research interests include wireless communications and statistical signal processing.

CHAO ZHANG (Senior Member, IEEE) received the B.S. and Ph.D. degrees from Beihang University, in 2001 and 2008, respectively. From 2008 to 2010, he was a Postdoctoral Fellow at the Department of Electronic Engineering, Tsinghua University, Beijing, China. He is currently an Associate Professor with the Department of Electronic Engineering, Tsinghua University. He has authored over 50 journal and conference papers. He holds over 20 Chinese patents. His research interests include wireless and visible light communications. He received the IEEE Scott Helt Memorial Award (Best Paper Award in IEEE TRANSACTIONS ON BROADCASTING), in 2016.

CHANGYONG PAN (Senior Member, IEEE) was born in Anhui, China, in 1975. He is a Full Professor with the Research Institute of Information Technology and the Deputy Director of the DTV Research and Development Center, Tsinghua University. He has authored or coauthored more than 180 technical papers and published eight technical books. He holds 34 patents. He was a recipient of the National Technical Award three times and numerous other awards.